ISSN 2176-5480

22nd International Congress of Mechanical Engineering (COBEM 2013)
November 3-7, 2013, Ribeirão Preto, SP, Brazil

EXPERIMENTAL RESULTS OF THE INTER-STAGE REGION OF SOUNDING ROCKET SONDA III IN A TRANSONIC WIND TUNNEL

João Batista Pessoa Falcão Filho
Maria Luísa Collucci da Costa Reis
IAE – Institute of Aeronautics and Space, Pça. Marechal Eduardo Gomes, 50, São José dos Campos – SP, CEP 12.228-904
jb.falcao@ig.com.br
mluisareis@yahoo.com.br

Guido Pires Arantes Ubertini
ITA – Instituto Tecnológico de Aeronáutica, Pça. Marechal Eduardo Gomes, 50, São José dos Campos – SP, CEP 12.228-901
guido_ubertini@hotmail.com

Abstract. *The Pilot Transonic Wind Tunnel (TTP) of the Institute of Aeronautics and Space (IAE) has been conducting a research project sponsored by the CNPq (National Counsel of Technological and Scientific Development – Brazil) to investigate the interference between the fins and the fuselage of the Sounding Rocket Aerospace Vehicle Sonda III. The aim of the investigation is to become better acquainted with the existing interference on the rocket inter-stage region in the presence of fins. A half-model of the Sonda III in scale 1:8 was built and installed on the side wall of the tunnel test section. The model has 49, 70 and 35 pressure taps distributed on the first-, second- and inter-stage, respectively, to analyze the pressure distribution near the inter-stage region. Experiments in sequence with increasing configuration complexity are being conducted (with no fins, with one fin perpendicular to the test section wall and with two fins positioned at 22.5 degrees in relation to the tunnel wall) in order to investigate the influence of the fins at various flow conditions. The tests will include variations in Mach number from 0.2 to 1.1, stagnation pressure from 0.5 bar to 1.2 bar and model angles of attack of 0, 5.5 and 8 degrees. This work shows some significant preliminary results undertaken with Mach numbers from 0.2 to 1.1.*

Keywords: *Transonic Wind Tunnel, Sounding Rocket, Sonda III, Interference, Fins*

1. INTRODUCTION

Transonic regimes which occur for a reasonably brief period during rocket flight present very important physical phenomena which have drawn the attention of researchers and designers because of their complexity. As the rocket proceeds through the atmosphere it will inevitably need to overcome the transonic regime, which is characterized by shock wave formation resulting in a huge drag increase and thereby requiring extra thrust from the engine. This difficulty was a real challenge for many decades for the aerodynamicists when they referred to the problem as the "sound barrier" (Becker, 1980). Actually the transonic regime is characterized by some supersonic regions inside a subsonic environment with interfaces that may be unstable, depending on many flow parameters and on the far-field boundary conditions. After surpassing the transonic regime the shock waves are more fully formed within a completely supersonic environment and the drag coefficient is reduced. The typical C_D0 (drag coefficient at zero angle of attack) curve presented in Fig. 1 shows the extensive drag increase in the transonic region. The drag coefficient is defined by Eq. (1) (Anderson, 2007)

$$C_D \equiv \frac{D}{q_\infty S} \tag{1}$$

where D is the drag force, S is a reference surface area and q_∞ is the freestream dynamic pressure defined by

$$q_\infty \equiv \frac{1}{2} \rho_\infty V_\infty^2 \tag{2}$$

where ρ_∞ and V_∞ are the freestream density and velocity.

Shock waves arise when the local speed along the vehicle's surface reaches Mach number 1 and this normally occurs at free flight subsonic speed. This is the reason why the C_D0 curve starts rising before the critical value of Mach number 1 in the undisturbed flight condition. The moment this starts depends on the shape of the vehicle. The way the shock wave develops and moves along the vehicle's surface is one of the most important phenomena in this speed regime. This is because the pressure variation across a shock wave is quite significant and its dislocation along the surface of the vehicle causes undesirable vibrations that will only disappear in full supersonic regime. For a manned vehicle the sonic regime can be reached in about 60 seconds and at an altitude as high as 10 km. For an unmanned

ISSN 2176-5480

vehicle this fact may occur much earlier. In general, the transonic range will happen during a very representative period of the mission and under very complex flow situations that require special attention from the technical team.

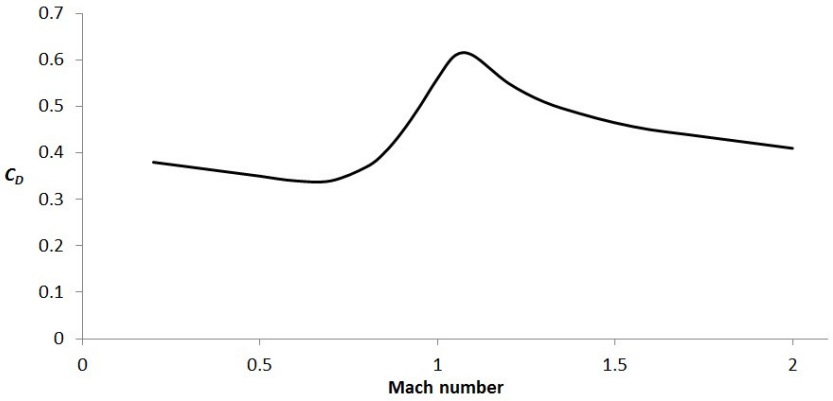

Figure 1. Curve of C_D0 for a typical rocket design

Experiments in transonic wind tunnels are very important to assess the flow characteristics of a vehicle by testing a scaled-down model in a controlled environment which is, as much as possible, representative of the real flight. The Pilot Transonic Wind Tunnel (TTP) of the Institute of Aeronautics and Space (IAE), installed in the Aerodynamic Division (ALA) has been used to test the vehicles designed in the Institute. The purpose of the tests is to obtain aerodynamic results utilizing a variety of measuring techniques: multi-component internal balances to determine the aerodynamic global forces and moments, pressure scanners and PSP technique (Pressure Sensitive Paint) to determine the pressure distribution on the model surface and ***Schlieren*** visualization system to obtain pictures from the flow field around the model (Falcão Filho ***et al.***, 2009). Figure 2 shows the aerodynamic circuit of the TTP.

Figure 2. View of the aerodynamic circuit of TTP 17 meters long

The tunnel has a test section which is 0.30 m wide and 0.25 m high, with automatic controls of Mach number, stagnation pressure (from 0.5 bar to 1.2 bar), temperature and humidity. It can operate continuously from Mach number 0.2 to 1.1 driven by a main compressor of 840 kW of power, but it can be run intermittently with the help of an injection system in combined action with the main compressor for about 30 seconds, reaching up to Mach number 1.3. Details about the TTP operation characteristics can be found in Falcão Filho and Mello (2002).

ISSN 2176-5480

TTP became fully operational in 2007 and in the same year the first campaign in the tunnel was carried out. A sounding rocket vehicle developed by the IAE, the Sonda III, was tested in a campaign financed by the AEB ("Brazilian Space Agency") from 2007 to 2010. A model available at the Institute which had not been tested in other tunnels was chosen as the test model basically because its dimensions were adequate for the size of the TTP test section.

The Sonda III vehicle is a two-stage sounding rocket developed by the Brazilian Institute of Aeronautics and Space (IAE) whose first stage has a diameter of 0.56 m and the second stage one of 0.30 m. It is capable of carrying a payload of approximately 100 kg up to an altitude of 600 km. It is one of the Brazilian sounding rocket family, which started with Sonda I, first launched in 1965. In 1996, the first stage of Sonda III was adapted to receive European experiments onboard (Reis *et al.*, 2009).

Figure 3 shows the two-stage Sonda III vehicle installed with the internal multi-component balance and ready for the tests in the TTP. Some results from this campaign can be found in Falcão Filho *et al.* (2010).

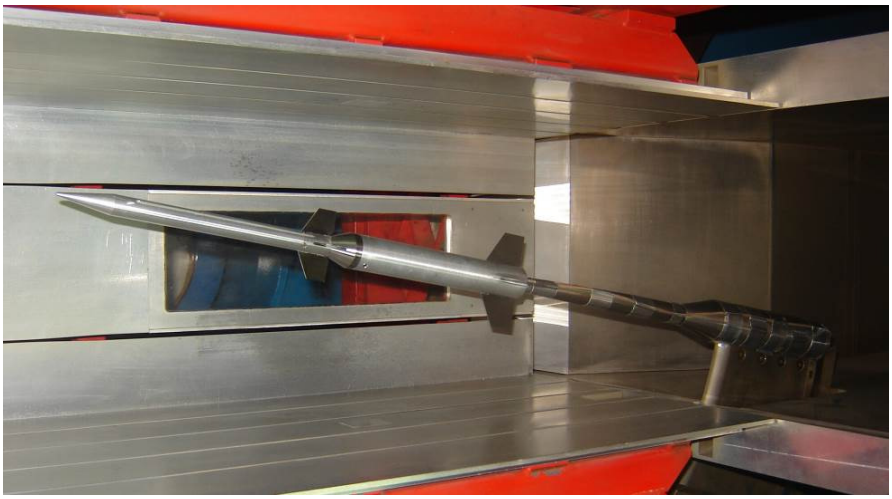

Figure 3. Sonda III model in scale 1:20 installed for tests in the test section of TTP, with multi-component internal balance

After performing the test campaign the idea of investigating the inter-stage region of the vehicle arose from the analysis of the collected results as it represents further advances in transonic tests research. With the financial backing of CNPq (The Brazilian National Counsel of Research and Development) the technical team started a new research project titled "Numerical/Experimental Analysis of the Sounding Vehicle Sonda III with Details of Interference Fin/Fuselage for Mach Number 1.3" to run from 2010 to 2014.

The present work describes the preliminary results obtained in the final phase of the project, with the development of tests undertaken with a half-model installed on the test section lateral wall of the tunnel. The aim of these tests is to determine the pressure distribution on the model in terms of the pressure coefficient defined by

$$C_P \equiv \frac{p - p_\infty}{q_\infty} \tag{3}$$

where p is the local pressure, p_∞ and q_∞ are the freestream static and dynamic pressures, already defined by Eq. (2).

2. DESCRIPTION OF MODEL DESIGN AND INSTRUMENTATION

In order to obtain more detailed results of the inter-stage region a larger scale model was idealized. In this case the bigger the model, the better. Because of the dimensional limits of the test section the model should be a half-model installed on the lateral wall of the test section. Figure 4 shows a 1:8 scale model, mounted on an Aluminum platform which will be fixed to the lateral wall of the tunnel test section. In Fig. 4 the model is configured with one fin perpendicular to the tunnel wall. Threads made in special places allow the model to change the direction in relation to the platform in order to adjust angles of attack of 0^o, 5.5^o, 8^o, 12^o, 13^o and 15.5^o. Between the half-model and the platform special spacers can be installed with the fixing screws to create a gap between the tunnel wall and the model. This way the possible boundary layer formed on the tunnel wall could be eliminated and would better represent the free flight situation.

The total length of the model is 0.778 m and the diameter of the first stage is 0.070 m. The dimensions of the second stage of the model were maintained but as the total length of model in scale 1:8 (0.984 m) would exceed the total length

ISSN 2176-5480

of the test section (0.810 m), the first stage was shortened. Probably there is no loss of the representativeness of the flow around the full scale counterpart because the aerodynamic phenomena of interest are upstream. The model was installed in such way to leave 0.100 m between the test section inlet section and the model tip, guaranteeing some space to adapt the flow. A model with these dimensions represents a problem as it greatly exceeds the so called nominal test section which has a length of 0.320 m. So, special attention has to be given to discern any kind of error or discrepancy from the data obtained during the tests.

Although the half-model is of a seemingly large dimension, its total blockage ratio is only 2.5%, which is not big enough to cause great effect on the opposite wall, as it is relatively distant.

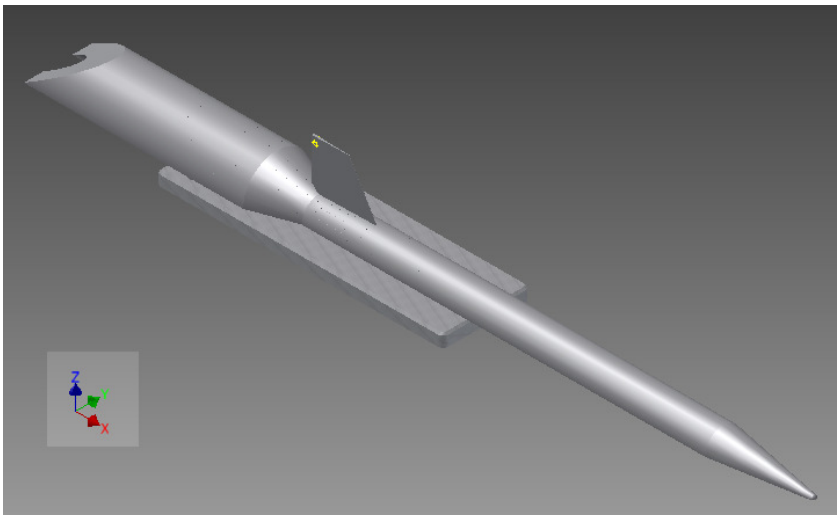

Figure 4. Model of Sonda III with scale 1:8 mounted on an Aluminum platform which will be fixed to the tunnel lateral wall

Figure 5 shows two complete drawing views of the model design, with the main dimensions. In the first view (Fig. 5 (a)) one can see the inner part of the model which will be mounted on the platform. There is a cylindrical hollow with 22 stations of 7 small holes circumferentially distributed – 154 holes in total. These holes are 2 mm in diameter. Each of them will be connected to a small hole made on the surface of the model. In the second view (Fig. 5 (b)) the external surface of the model with holes of 0.5 mm in diameter perpendicular to the surface is shown. Each hole on the surface of the model is connected to a 2 mm hole in the inner part of the model.

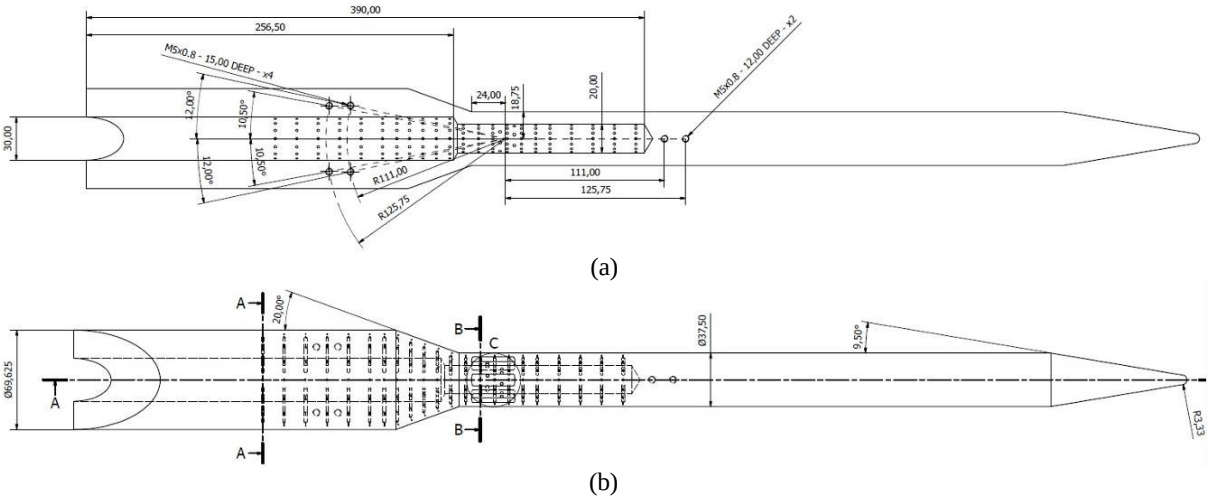

Figure 5. The model views: (a) inner part; (b) outer part, with 154 measuring pressure taps

Figure 6 shows some details of the model design. In Fig. 6 (a) one can see the inter-stage region with 5 stations on the frustum cone part – the 0.5 mm pressure taps had to be connected to the 2.0 mm holes with an angle of 20°. Observe

ISSN 2176-5480

how close one of the tap stations is to the bigger diameter of the frustum cone. Figure 6 (b) shows how the seven taps at a determined station are circumferentially distributed, at intervals of 22.5°, with one at a perpendicular direction in relation to the wall plane. Figure 6 (c) shows how the 22 measuring stations are distributed along the stream-wise direction: 7 in the first stage, 5 in the frustum cone and 10 in the second stage. Close to frustum cone the distance between the stations is 10 mm while far from the inter-stage region the distance is 15 mm, ensuring a better assessment of the region of interest. Each measuring station was nominated by a letter, starting with "A" on the left (at 132.00 mm from the aft end) to "V" on the right (384.13 mm from the aft end) (in Fig. 6 (c)), and each of the seven pressure taps was numbered from 1 to 7 from top to bottom. So, for example, the pressure tap M3 stands for the third pressure tap from top to bottom at the 13th measuring station – this particular example is the first measuring station of the second stage of the model. Each number, from 1, 2, 3, 4, 5, 6 and 7, corresponds to the angle in relation to the perpendicular direction. Holes are 22.5° apart from each other.

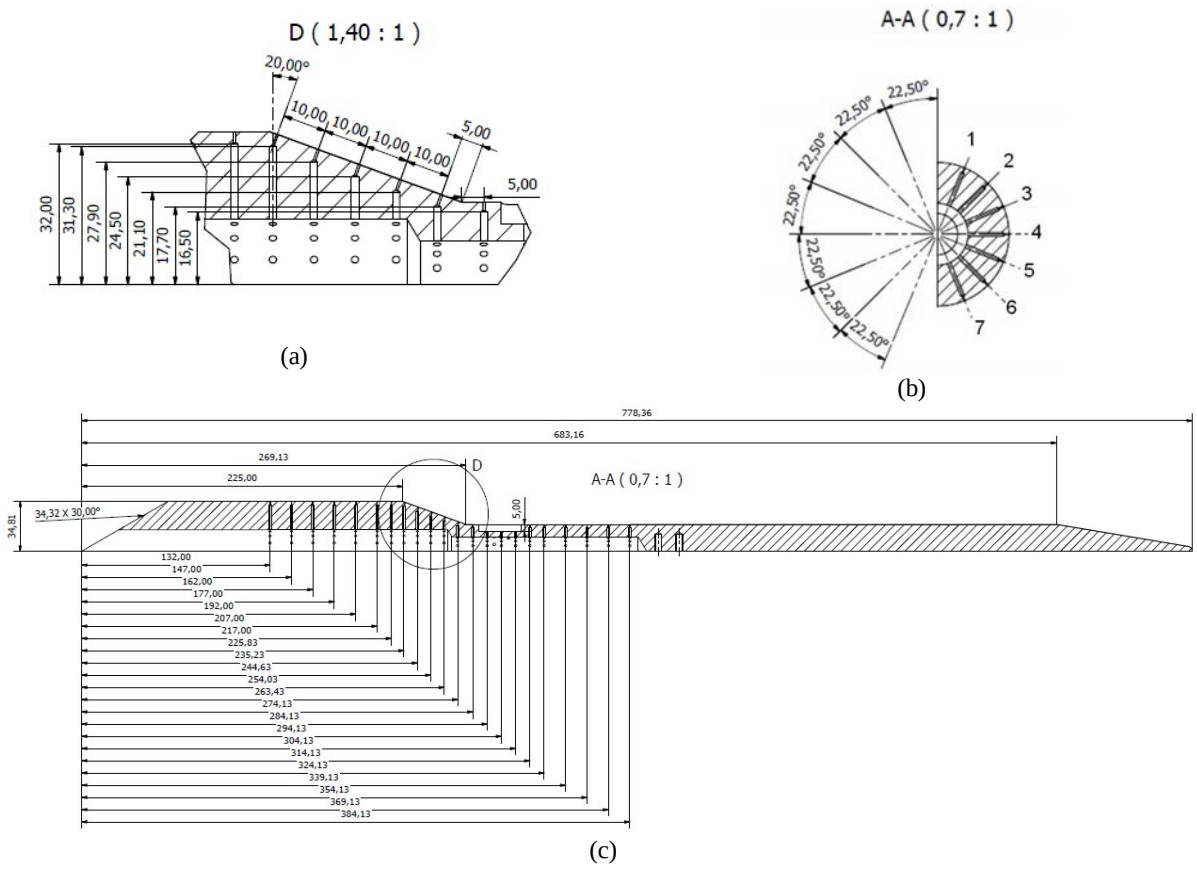

Figure 6. Details of the model design: (a) the inter-stage part with the hole connections; (b) the 7 holes circumferentially distributed in one station; (c) the 22 longitudinally distributed measuring stations

Figure 7 (a) shows the Sonda III model with details of the plastic tubes connected to each of the 154 measuring places. The plastic tubes were connected without leaving any space around the holes as they have the same outer diameter and later, permanent glue was applied to each connection. Each measuring point was tested to guarantee a proper operation. In this figure one can see the region where the fins are attached. There are three housings at angles of 45°, 90° and 135° to install the fins in two different configurations: with one fin at 90° and two fins at 45° and 135°. The fins are mounted on small bases which are installed in the corresponding housings. There are bases to mount the fins aligned at 0°, 2.5° and 5.0° with the stream-wise direction, making it possible to test all the configurations present in the original Sonda III scale model 1:20. If no fin is installed on a particular mounting, a blunt base is installed instead. The blunt base allows three pressure taps to communicate pressure through it from the surface to the inside of the model. Figures 7 (b) and (c) show these two configurations with one and two fins, respectively. The model also permits the configuration with no fins, with three blunt bases installed. During the campaign all situations will be tested, changing the number and the angle of the fins, as well as the angle of attack of the model.

ISSN 2176-5480

(a)

(b)

(c)

Figure 7. Sonda III model with detail of the plastic tubes connected and the housings for the fins empty (a), and the model with the fins in two different configurations: (b) one fin at 90°, two fins at 45° and 135°.

Figure 8 (a) shows the complete installation of the Sonda III model with no fins on the lateral wall of the tunnel and ready to be installed. The present work presents preliminary results of the configuration with no fins and at zero angle of attack. The model was installed with spacers in the fixing screws to allow a gap of 4 mm between the tunnel wall and the model as shown in Fig. 8 (b).

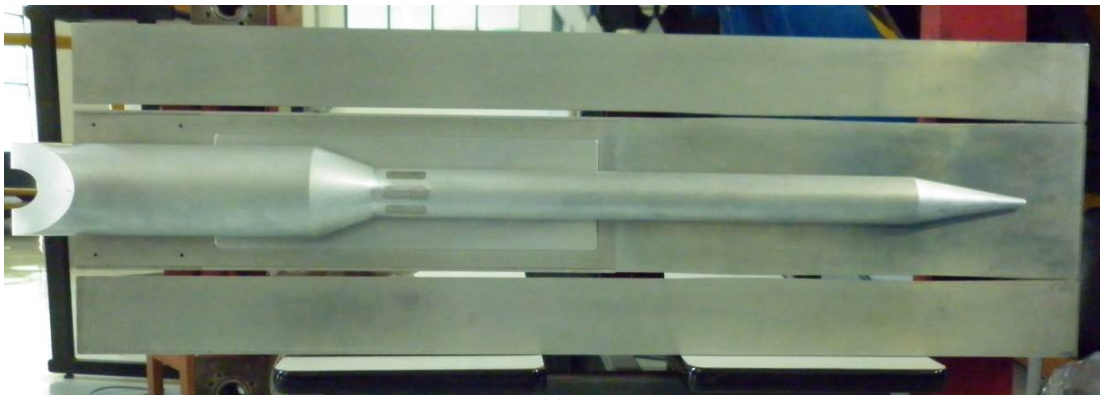

(a)

(b)

Figure 8. The complete installation of the Sonda III model (scale 1:8) on the lateral wall of the test section with no fins (a) and detail of the gap of 4 mm between the model and the wall (b)

ISSN 2176-5480

Each pressure measuring point was connected by means of plastic hoses to a pressure scanner in contact with the local atmosphere. The pressure scanner module used was from PSI – "Pressure Sensor Instruments" (PSI, 2000), consisting of 32 differential pressure channels with a pressure range from –10 to +10 psi. During the run a stable control condition of the flow parameters was established before starting the acquisition which lasted about 60 seconds. A high precision absolute pressure sensor from TESTO (TESTO, 2000) was used to recover the actual pressure level from the differential pressure read in the pressure module. The acquisition system is controlled and monitored on a micro-computer by a special software developed in LabView© platform.

3. EXPERIMENTAL RESULTS

The tests were performed with the model configured without fins. These preliminary tests were very important to check the effectiveness of the gap created between the test section wall and the model in reducing the effects of the boundary layer. Furthermore, they were fundamental to obtaining a first pressure distribution along the model surface at various flow conditions.

Two tests were executed. In the first test the effectiveness of the gap was verified by measuring the pressure distribution in the circumferential direction. The pressure taps from three different measuring stations were chosen: A, R and V, at 132 mm, 354 mm, and 384 mm from the aft end of the model (see Fig. 6 (c)). In the second test all central pressure taps at each station were chosen to obtain the pressure distribution along the stream-wise direction.

Table 1 shows the resulted parameters related to the test section entrance, read from the control system of TTP for each run of the two tests performed, which means they are considered as undisturbed flow condition parameters. The standard deviation was determined directly from the values of the parameters during the period considered in each run. One can observe that runs 9 and 10 of the second test were for the same nominal Mach number value – test number 9 was repeated with increased dryer operation, guaranteeing a lower dew point and avoiding condensation. This condition was used in the following runs, although the results from runs 9 and 10 were practically the same, demonstrating that the original dryer operation was already sufficient.

Table 1. Parameters of the tests performed in TTP, obtained from the control system.

Run	Mach Number	Stagnation Pressure (Pa)	Stagnation Temperature (K)
FIRST TEST – circumferential measuring in stations A, R and V			
1	0.4008 ± 0.0007	93,929 ± 37	301.5 ± 0.1
2	0.5993 ± 0.0006	93,947 ± 52	300.9 ± 0.1
3	0.7984 ± 0.0006	93,932 ± 55	305.8 ± 0.2
4	0.8486 ± 0.0007	93,956 ± 31	307.0 ± 0.1
SECOND TEST – longitudinal measuring in all stations			
1	0.1999 ± 0.0012	93,918 ± 19	293.8 ± 0.1
2	0.3004 ± 0.0008	93,978 ± 24	294.6 ± 0.1
3	0.3998 ± 0.0010	93,968 ± 29	295.7 ± 0.1
4	0.4997 ± 0.0008	93,910 ± 44	297.6 ± 0.2
5	0.6003 ± 0.0006	93,875 ± 38	299.2 ± 0.1
6	0.7006 ± 0.0008	93,864 ± 60	301.1 ± 0.1
7	0.7991 ± 0.0006	93,902 ± 42	303.7 ± 0.1
8	0.8463 ± 0.0006	93,818 ± 74	305.5 ± 0.1
9	0.8996 ± 0.0009	93,896 ± 83	306.6 ± 0.1
10	0.8998 ± 0.0006	93,987 ± 124	307.1 ± 0.1
11	0.9501 ± 0.0012	93,905 ± 53	308.4 ± 0.1
12	0.9986 ± 0.0007	93,911 ± 85	309.3 ± 0.1
13	1.0511 ± 0.0008	93,912 ± 39	310.3 ± 0.1
14	1.0984 ± 0.0005	93,874 ± 81	311.4 ± 0.1

Figure 9 shows the results from the first test for Mach numbers 0.4, 0.6, 0.8 and 0.85. The measuring points at the three chosen stations are represented in the figure as diamonds (station A), squares (station R) and triangles (station V). One can see how uniform the pressure values are in all circumferential direction, indicating that the gap of 4 mm created between the test section wall and the model practically cancelled the boundary layer effects over the half-model

ISSN 2176-5480

fuselage. However, a thorough investigation by varying the gap dimension to find an optimized solution will be performed later.

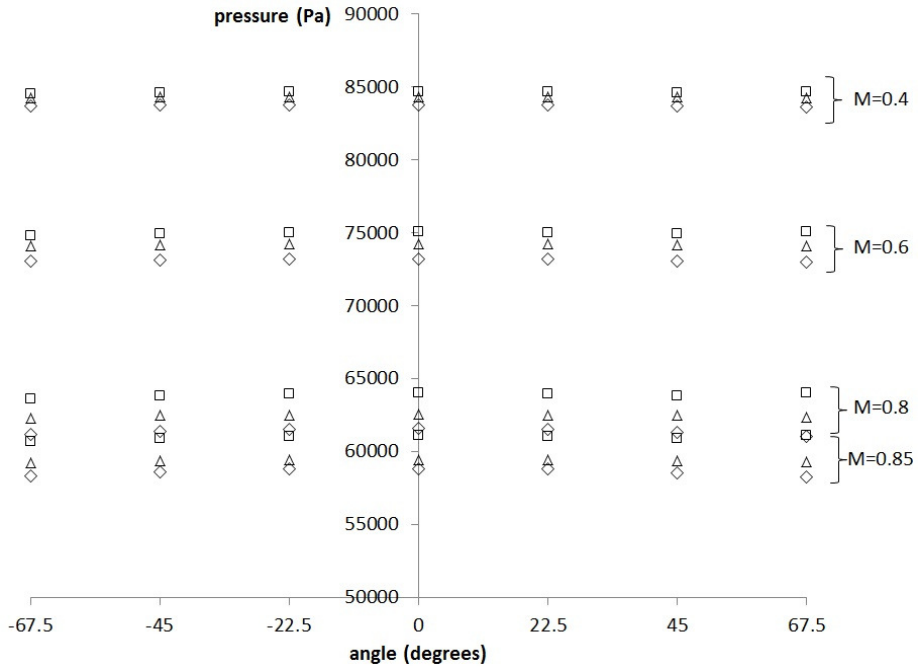

Figure 9. Pressure values from the first test, at the measuring stations A (diamonds), R (squares) and V (triangles) for various Mach numbers

Although the values of the standard deviation were relatively low, a careful view is appropriate. Figure 10 shows the spatial pressure standard deviation for each Mach number at each measuring station. At Mach number 0.4 at all the measuring stations the standard deviation was lower than 50 Pa, which is practically the precision of the instrument, but the values increased as the Mach number increased. One can observe the low standard deviation values at the measuring station V, which is the first station to receive the flow entering the test section. At station R, only a little after the V position, the standard deviation was already high. At the last measuring station (at the end of the model) the standard deviation was high for high Mach number condition. These facts indicate that a better research for optimizing the gap dimension is desirable.

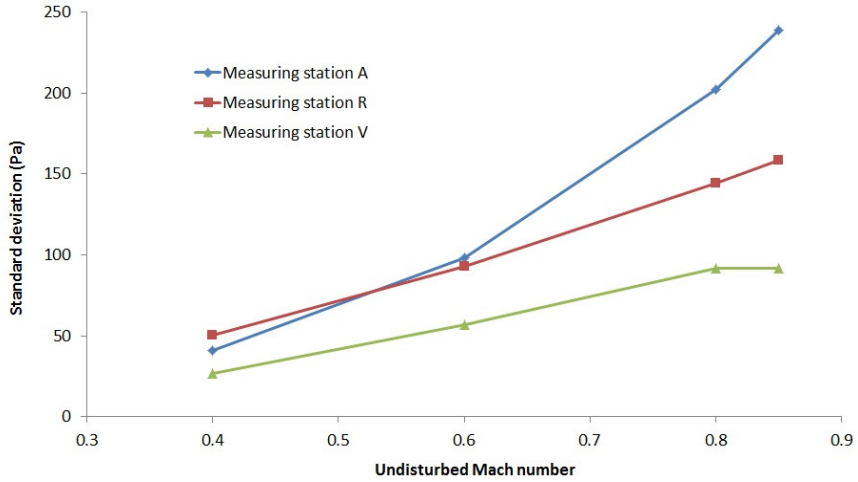

Figure 10. Spatial (circumferentially) standard deviation of pressure value for three measuring stations with Mach number variation

ISSN 2176-5480

As it was proven that the pressure values are practically independent of the circumferential position of the measurements, the second test aims to determine the longitudinal pressure distribution over the model surface. In this test, because of the limited number of pressure channels available for acquisition, only one pressure tap at each measuring station was used – the pressure tap in the direction perpendicular to the test section wall (90°).

Figure 11 shows all the results in a single plot. The $-C_P$ curves for each Mach number, according to the runs in Table 1, were plotted in such a way to shift the curves one from the other for the sake of clarity. The only curve that was not shifted was the first one, corresponding to Mach number 0.2. Because of the shift of the curves, the ordinate axis is not representative, and that is why it was not plotted. Each experimental value of the coefficient of pressure was plotted as a marked point, and the points along the model for the same Mach number condition were joined by solid lines.

In the longitudinal direction the positions are plotted in such a way that the origin coincides with the minor diameter of the frustum cone. A schematic representation of the region of the model where the measurements were taken was also drawn at the bottom of the graph, highlighting the initial and the final sections of the frustum cone with vertical dashed lines.

One can observe from the figure the effect of the frustum cone, which increases the pressure level before reaching it (indicated by the decrease of $-C_P$), in the second stage region. For a supersonic regime this effect is accentuated probably due to the presence of a detached shock wave ahead of the frustum. It is worth mentioning that behind a detached shock wave the aerodynamic phenomenon is very complex (Zucker and Biblarz, 2002).

The five measuring points in the frustum cone indicate, except in the case of Mach number 1.1, an acceleration denounced by the continuous increase of $-C_P$ values. After the frustum cone (after the second dashed line) the pressure increases or decreases, depending on the nominal Mach number. For the first 5 curves (from Mach number 0.2 to 0.6) the pressure rises ($-C_P$ decreases) after the frustum cone. Starting at curve number 6 (corresponding to Mach number 0.7) the pressure decreases ($-C_P$ rises) and this fact is even more intense at higher Mach numbers. This indicates the strong effect of the expansion in this position at supersonic regime.

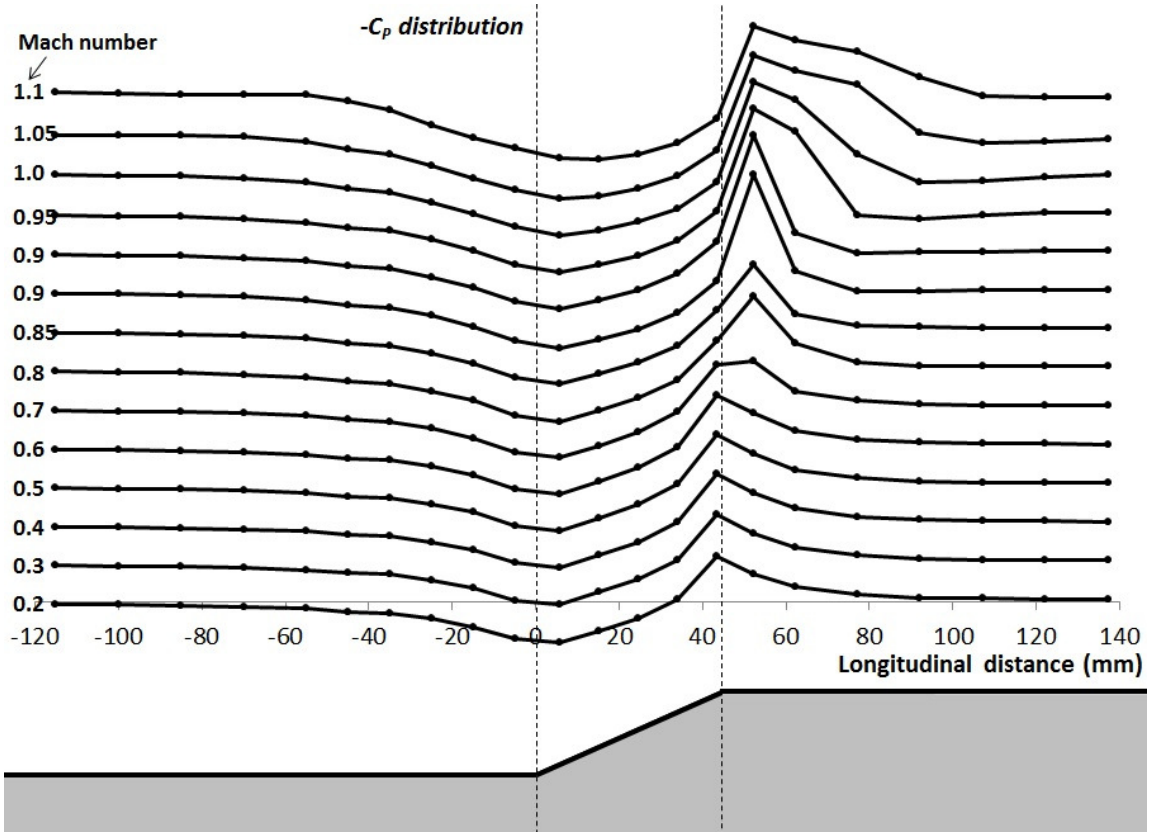

Figure 11. Curves of the coefficient of pressure ($-C_P$) distribution along the model surface. The curves are for all 14 runs according to Table 1, from Mach number 0.2 to 1.10. Starting with the curve corresponding to Mach number 0.3 the curves were shifted for clarity, so the ordinate axis was not plotted.

After reaching supersonic regime by the expansion process, the pressure returns to its original value due to the presence of a shock wave. This fact is very clear at Mach number 0.9 regime where one can see an abrupt pressure drop

ISSN 2176-5480

after the expansion (first point after second dashed line), followed by a pressure rise after the shock wave (second point after the second dashed line). Considering the same stagnation pressure of the test section, the local pressure reading resulted in local Mach number of 1.45 at the first point (in the expansion region). This particular run was repeated (runs number 9 and 10 in Table 1) and the same pressure distribution was obtained.

As the Mach number rises above 0.9 the expansion region seems to increase and the shock wave occurs at a more distant location. For example, for Mach number 1.1 it is possible to see that the pressure only recovers four measuring points after the expansion occurs. However, this recovery process was smoother than the one observed at Mach number 0.9. Probably there is a very complex situation in this area with three-dimensional expansion effects that should be investigated in the future.

4. CONCLUSIONS

The preliminary tests undertaken with the model of the Sonda III in scale 1:8, with details of the frustum cone in the inter-stage, were developed in the Pilot Transonic Wind Tunnel.

This work represents the final phase of the development which was started in 2007 with the first tests performed using the Sonda III model of scale 1:20. It describes the main parts of this development concluding with this new model. The design details are presented as well as the instrumentation utilized in the tests.

Initially, the gap effectiveness between the tunnel wall and the model was verified in terms of the pressure distributed circumferentially in the model, and the selected gap has been proven adequate. It was observed that measured pressure values presented uniformity at all pressure taps belonging to the same measuring station. Later the model was tested at all Mach numbers ranging from 0.2 to 1.1 to obtain the $-C_P$ distribution along the stream-wise direction. The results were within expectation and proved that the semi-model configuration is able to provide quality results about the Sonda III sounding rocket. They also pointed to some further research that needs to be done in order to fully comprehend the complex situations detected in the inter-stage section of the model.

5. ACKNOWLEDGEMENTS

The authors would like to express their gratitude to CNPq, the Brazilian Counsel of Research and Development for their help during the development of this work through grant 560200/2010-2 and the individual support number 381448/2011-8.

6. REFERENCES

Anderson, J. D. Jr., 2007, *Fundamentals of Aerodynamics*, McGraw-Hill International Edition, Forth Edition.

Becker, J. V., 1980, "The High Speed Frontier – Case Histories of Four NACA Programs, 1920-1950", NASA Scientific and Technical Information Branch, National Aeronautics and Space Administration Washington, DC, NASA SP-445.

Falcão Filho, J. B. P., Avelar, A. C., Reis, M. L. C. C., 2009, "Historical Review and Future Perspectives for the PTT – IAE Pilot Transonic Wind Tunnel," *Journal of Aerospace and Technology and Management*, ISSN 1984-9648,Vol. 1, No. 1, Jan-Jun 2009.

Falcão Filho, J. B. P., Mello, O. A. F., 2002, "Descrição Técnica do Túnel Transônico Piloto do Centro Técnico Aeroespacial," Anais ... IX Congresso Brasileiro de Ciências Térmicas e Engenharia, ENCIT-2002, Caxambu-MG, artigo CIT02-0251.

Falcão Filho, J. B. P., Reis, M. L. C. C., Morgenstern, A. Jr., 2011, "Experimental Results from the Sounding Vehicle Sonda III Test Campaign in the Pilot Transonic Wind Tunnel," *Journal of Aerospace and Technology and Management*, doi: 10.5028/jatm.2011.03033111 ISSN 1984-9648, ISSN 2175-9146 (online), Vol.3, No.3, pp. 311-324.

PSI, 2000, "ESP-16BP Pressure Scanner User´s Manual," catálogo de produto da firma Esterline Pressure Systems 3rd Edition – www.pressuresystems.com.

Reis, M. L. C. C., Falcão Filho, J. B. P., Paulino, G., Truyts, C., 2009, "Aerodynamic Loads Measurement of a Sounding Rocket Vehicle Tested in Wind Tunnel," XIX IMEKO World Congress, Fundamental and Applied Metrology, September 6/11, 2009, Lisbon, Portugal.

Testo, 2000, "Instrumentos Portáteis de Medição", catálogo de produto da firma Testo do Brasil Instrumentos de Medição Ltda. – www.testo.com.br.

Zucker, R. D., Biblarz, O., 2002, *Fundamentals of Gas Dynamics*, John Wiley and Sons Inc., 2nd ed.

7. RESPONSIBILITY NOTICE

The authors are the only responsible for the printed material included in this paper.